(Received 14 April 2023, Accepted 27 November 2023, Scheduled 9 September 2024)

# Multi-Band Band-Pass Filter with Independently Controlled Asymmetric Dual-Band Response Based on Metacell

Shobha Hugar[1,*], Jambunath Baligar[2], Veerendra Dakulagi[3], and K. M. Vanitha[4]

[1] *Department of Electronics and Communication Engineering, Sapthagiri College of Engineering, Bangalore, India*
[2] *Department of Electronics and Communication Engineering, Dr Ambedkar Institute of Technology, Bangalore, India*
[3] *Department of Electronics and Communication Engineering, Guru Nanak Dev Engineering College, Bidar, Karnataka, India*
[4] *Department of Electronics and Instrumentation Engineering, M S Ramaiah Institute of Technology, Bangalore, India*

**ABSTRACT:** The key challenges in the design of multi-band filters are realizing highly independent, controlled asymmetric-wide and narrow dual-band response. To address these challenges this paper proposes the design and development of a dual-band band-pass filter (BPF) with highly independent, controlled wide and narrow band responses. The proposed filter is constructed using only two resonator structures, asymmetric step impedance resonator (A-SIR) and metacell. The wide and narrow band responses are independent and are controlled independently by impedance ratio (R) and the number of cells (N) in metacell structure, respectively. Additionally quasistatic circuit model of the metacell is used to analyze independently controlled narrow passband response. The prototype of the filter is fabricated, and the simulation results are validated through experimental measurements.

## 1. INTRODUCTION

The rapid development of multiple frequency systems, such as carrier aggregation or wireless local area network (WLAN) bands, has created a demand for compact, high performance, high-Q, multi-band filters with independently controlled wide and narrow asymmetric dual-band responses. In recent years, many researchers have focused on the design of multi-band filters using different resonator structures [1–12]. Using symmetric open-circuited stub-loaded resonators, a dual-band filter with fractional bandwidths of 6.5% and 4.3% centered at 3.5 GHz and 5.23 GHz has been designed in [1]. A tri-band BPF has been proposed using two symmetrical stub loaded step impedance resonators (SLSIRs) separated by a short circuited stub in [2]. Cross resonators have also been used to implement multi-band filters [3, 4]. Using wider fractional bandwidth characteristic of the cross stub step impedance resonator (CS-SIR), a wide dual-band filter with fractional bandwidths of 94.19% and 33.52% has been designed in [3]. A crossed resonator consisting of a central resonator, a short stub, and an open stub shunted at the resonator center has been used to successfully implement triple band filter [4]. To reduce the size of multi-band filters, a meander coupled line resonator structure has been proposed and investigated [5]. As a result, the size of multi-band filter has been drastically reduced, but passband responses are dependent. High-temperature superconducting resonators (HTSs) and substrate-integrated waveguide (SIW) resonators [6, 7] have also been proposed to implement multi-band filters. However, these methods have manufacturing difficulties, and passband responses are also interdependent. Multimode resonators such as stub loaded SIR [8], quarter-wavelength SIR [9], asymmetric SIR [10], coupled-line SIR [11], and trisection SIR [12] have been the most promising structures for designing multi-band filters and have shown good performance parameters such as good insertion loss and reflection coefficient. However these filters have large size and generic, interdependent multi-band response. Reconfigurable dual-band filters proposed in [13–15] have conventional, highly dependent dual-band responses, and above all these filters require additional switching components — radio frequency (RF) micro-electromechanical system (MEMS) switches, piezoelectric IC sensors, and memristive switches. Lu et al. in [16] have used separate electric and magnetic coupling to implement a highly independent response dual-band filter. An independent multi-band filter proposed by Chu et al. in [17] has high insertion loss. All multi-band filters proposed in [1–15] have generic, highly dependent multi-band responses, and moreover the responses are not controlled independently. The dual-band BPFs proposed by Weng et al. in [18] and Huang et al. in [19] have narrow and wide dual-band responses, but the responses are not controlled, and the dependency of response is not discussed.

In this paper, we extend our previous work [20] where we discussed in detail the design of a wide and narrow asymmetric response dual-band BPF based on metacell. However in this paper, we have propose the design of a highly independent, controlled wide and narrow response dual-band BPF. The proposed filter is designed and fabricated on a dielectric substrate RT/Duroid 5870 which has a relative dielectric constant ($\varepsilon_\mathbf{r}$) of 2.55, thickness ($h$) of 0.0762 cm, and tangential loss ($\delta$) of 0.0009.

* Corresponding authors: Shobha Hugar (shobha_hugar@yahoo.co.in).

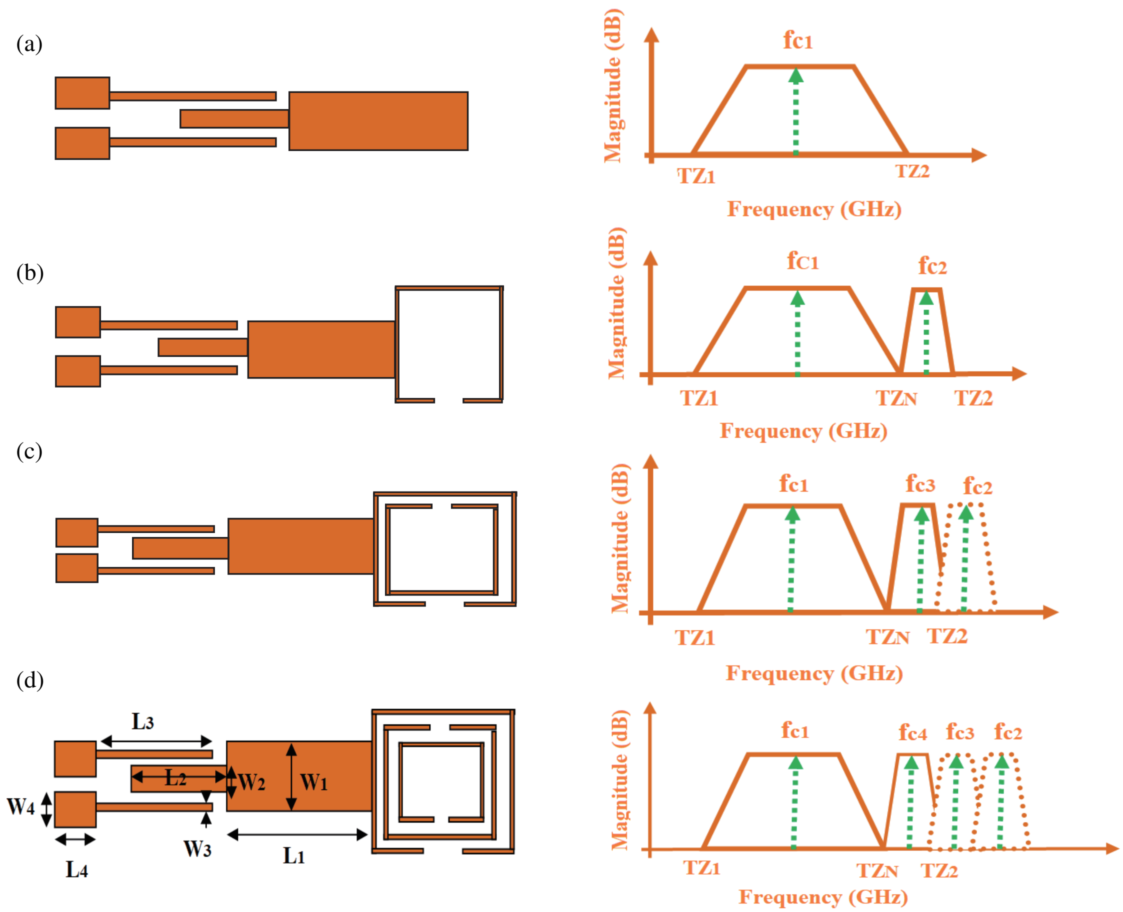


**FIGURE 1**. Filter structures and conceptual responses. (a) wide bandpass filter and its response (b) wide and narrow dual-band filter and its dual-band response (c)–(d) independently controlled dual-band filters and their responses .

## 2. METHOD

The filter structures shown in Figs. 1(a) and (b) realize single wideband and dual wide and narrow band responses [20], respectively. Figs. 1(c)–(d) depict structures of proposed highly independent controlled wide and narrow dual-band filters. Here, highly independent controlled filter means that wide and narrow passband responses are independent and are controlled independently. In the proposed work, we have shown that narrow passband performance is independently controlled without affecting the performance of wide passband. The wide and narrow multi-band performance is produced by using two resonator structures: A-SIR and metacell resonator structures with multiple rings. The A-SIR is designed for wide passband frequency ($f_{\mathbf{C1}}$) and impedance ratio (R) greater than unity. In Figs. 1(c) and (d), the wide passband response ($f_{C1}$) can be controlled independently by varying the impedance ratio ($R$) of A-SIR, and the narrow passband ($f_{C2}$) can be controlled independently by varying the number of rings ($N$) in the metacell structure.

The significant contributions of our work are as follows:

1) Most of the multi-band filters reported in the literature have generic dual-band performance, and the responses are also interdependent. As a novelty, our work aims at wide and narrow multi-band response, and each passband response is independent.

2) Each passband response can be controlled independently or separately.

3) The response of wide passband ($f_{C1}$) can be controlled independently by varying the impedance ratio ($R$) of A-SIR.

4) The response of the narrow passband ($f_{C2}$) can be controlled independently by varying the number of rings ($N$) in the metacell.

5) The insertion loss ($S_{21}$) less than 1 dB in both the passbands is achieved by selecting an A-SIR structure with single step discontinuity as a basic resonator structure to design the proposed filter.

6) Steep skirt dual-band performance is achieved successfully to avoid interference with other bands by using a tightly coupled feeding method.

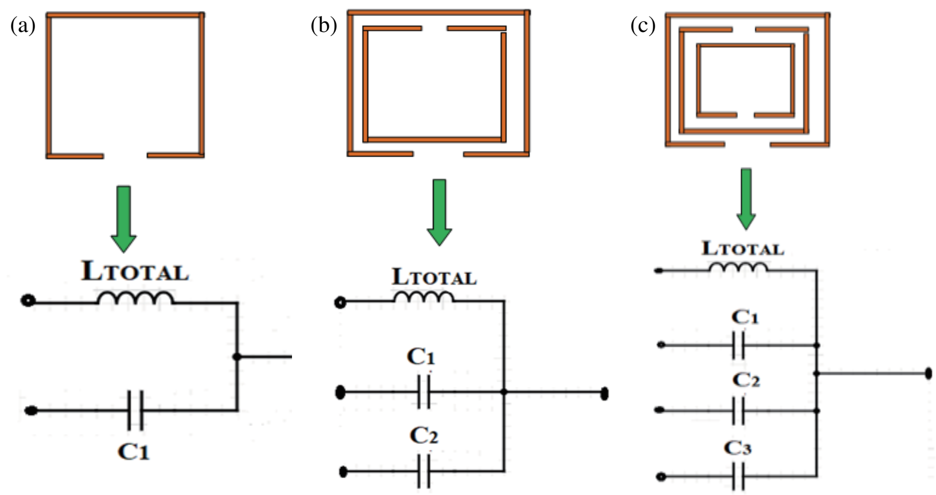


**FIGURE 2**. Metacell structures and qusistatic models, (a) single ring cell, (b) doublering cell, (c) triplering cell.

## 3. INDEPENDENT CONTROL OF NARROW PASSBAND ($f_{C2}$)

In the proposed dual-band filter, the narrow passband frequency ($f_{C2}$) is independent of the wide passband frequency ($f_{C1}$) and can be controlled independently by varying the number of rings ($N$) in the metacell structure. To obtain an insight on the dependency of narrow passband frequency ($f_{C2}$) on the number of rings ($N$) in the cell, the quasistatic model of the metacell for multiple rings is analyzed. The models for single, double, and triple rings metacells are shown in Fig. 2.

The metacell is a parallel resonator circuit, and its resonant frequency ($f_r$) is given by $f = \left(2\pi\sqrt{LC}\right)^{-1}$. For the metacells shown in Figs. 2(a), (b), and (c) with single, double, and triple rings, the resonant frequencies are expressed by Eqs. (1), (2), and (3), respectively [21]

$$f_1 = \left(2\pi\sqrt{L_{TOTAL}C_1}\right)^{-1} \quad (1)$$

$$f_2 = \left(2\pi\sqrt{L_{TOTAL}\left(C_1 + C_2\right)}\right)^{-1} \quad (2)$$

$$f_3 = \left(2\pi\sqrt{L_{TOTAL}\left(C_1 + C_2 + C_3\right)}\right)^{-1} \quad (3)$$

From Eqs. (1)–(3) it is very clear that as the number of rings in the cell structure increases, the distributed capacitances ($C_1$, $C_2$, $C_3$) increase, and resonant frequency ($f_r$) drops. As a result, a shift in the location of only narrow passband frequency ($f_{C2}$) is observed without disturbing the location of wide passband frequency ($f_{C1}$). The effect of the number of rings (N) on the resonant frequency of the cell is also studied by ADS simulation where single, double, and triple ring cell structures are simulated. From the simulation results it is observed that the total distributed capacitance ($C_{\mathbf{TOTAL}} = C_1 + C_2 + C_3$) increases for $N \leq 3$. With a further increase in $N$, the distributed capacitance associated with inner rings is less significant as shown in Fig. 3(a).

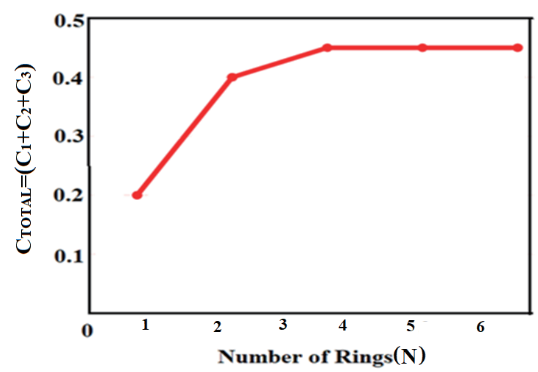


**FIGURE 3**. $C_{\mathbf{TOTAL}}$ as a function of the number of rings ($N$).

## 4. SIMULATION RESULTS

Figure 4(a) shows the circuit model for the proposed highly independent, controlled wide and narrow dual-band BPF. The dimensions of the proposed BPF after optimization using the ADS software are given in Table 1. The performances of the proposed filter verified by the simulation and simulation results are shown in Figs. 4(b)–(c). As shown in Fig. 4(b), a new transmission zero is realized at 5.2 GHz which is the resonant frequency of the single ring metacell, and a wide and narrow dual-band response is achieved. The wide passband is centered at 3.3 GHz, and the narrow passband is centered at 5.8 GHz. The addition of double and triple ring metacell structures shifts the location of the new transmission zero from 5.2 GHz to 5.1 GHz and 5 GHz, respectively. This shift in location of $TZ_N$ results in a shift in location of only the narrow passband frequency from 5.8 GHz to 5.7 GHz and 5.6 GHz, respectively, without disturbing the wide passband frequency as shown in Fig. 4(b). The reflection coefficient ($S_{11}$) in both passbands is more than 10 dB in all cases ($N = 1, 2, 3$) as shown in Fig. 4(c). Both wide and narrow passbands have transmission loss less than 1 dB indicating minimum signal attenuation. The transmission zeros at 1.5 GHz and 6.3 GHz with attenuation levels of 67 dB an 54 dB respectively provide good frequency selectivity for both

**TABLE 1**. Optimized dimensions of the presented filter in mm.

| $L_1$ | $L_2$ | $L_3$ | $L_4$ | $l_1$ | $l_2$ | $l_3$ |
|---|---|---|---|---|---|---|
| **10.2** | **15** | **19** | **1** | **17** | **14** | **7** |
| $W_1$ | $W_2$ | $W_3$ | $W_4$ | $g$ | $s$ | |
| **3.2** | **0.3** | **0.2** | **1.5** | **1.2** | **0.1** | |

(Note: $l_1$ ,$l_2$, $l_3$ are lengths of outer, middle and inner square rings in the cell$s$ is the spacing between the cells and is constant. $g$ is the split gap in each cell and is constant.)

**TABLE 2**. Comparison of simulation and experimental results.

| Parameters | Single ring metacell | | Double ring metacell | |
|---|---|---|---|---|
| | Sim | Pra | Sim | Pra |
| Wide passband frequency | 3.4 GHz | 3.45 GHz | 3.4 GHz | 3.45 GHz |
| Narrow passband frequency | 5.8 GHz | 5.89 GHz | 5.7 GHz | 5.74 GHz |
| $S_{11}$ (dB) | >10 dB | >10 dB | >10 dB | >10 dB |
| $S_{21}$ (dB) | <1 dB | <1.5 dB | <1 dB | <1.5 dB |

**TABLE 3**. Performance comparison with other multi-band filters reported in the literature.

| **Ref** | **Passbands (GHz)** | **Passband BW** | **FBW%** | **Independent, controlled passband** | **Size** $\lambda_g * \lambda_g$ |
|---|---|---|---|---|---|
| [22], 2018 | 2.4/5.7 | Narrow/Narrow | — | No | $0.02\ \lambda_g^2$ |
| [23], 2020 | 3.6/5.7 | Narrow/Narrow | — | No | $0.19 * 0.11$ |
| [24], 2018 | 2.45/5.85 | Narrow/Narrow | 32.3/10.5 | YES | —- |
| [25], 2019 | 1.57/2.38 | Narrow/Narrow | 9.9/6.5 | No | $1.1 * 0.48$ |
| [26],2020 | 7.6/11.5 | Wide/Narrow | 78.9/2.34 | No | $0.198\ \lambda_g^2$ |
| [27], 2019 | 0.9/2.25 | Narrow/Wide | 8/39 | No | $0.48 * 0.09$ |
| [28], 2018 | 0.9/2.25 | Narrow/Narrow | 6.4/4.4 | No | $0.28 * 0.23$ |
| **This work** | **3.3/5.7** | **Wide/Narrow** | **72/2.6** | **YES** | $\mathbf{0.58 * 0.122}$ |

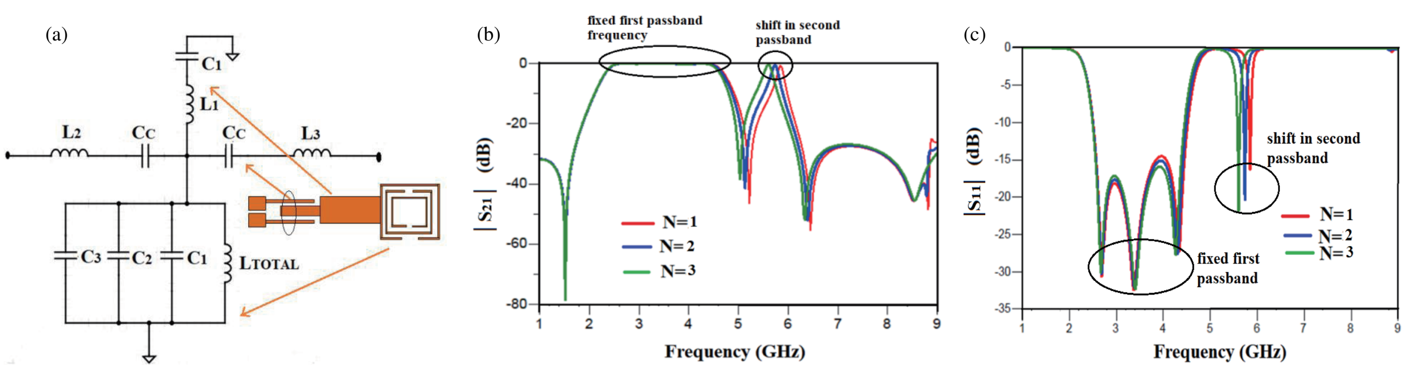


**FIGURE 4**. Circuit model and simulation results (a) lumped circuit for independent,controlled wide and narrow dual-band BPF (b) $S_{21}$ response (c) $S_{11}$ response.

passbands. These simulation findings have shown that only the narrow passband frequency ($f_{C2}$) can be controlled independently by varying the number of rings in the metacell structure, while wide passband response is completely independent of the narrow passband. This study also demonstrates that with an increase in the number of rings in the cell, the resonant frequency of the cell decreases, and consequently the narrow passband frequency decreases from 5.8 to 5.7 GHz.

## 5. EXPERIMENTAL RESULTS

For experimental validation, the proposed highly independent, controlled wide and narrow multi-band BPF is fabricated with single and double rings in the metacell structure. Photographs of the fabricated filters are shown in insets of Fig. 5(a). The practical responses are compared with simulation ones in Figs. 5(a)–(b) and are tabulated in Table 2. Finally, in Table 3 the performance of the proposed filter is compared with that of some multi-band filters reported recently in literature.

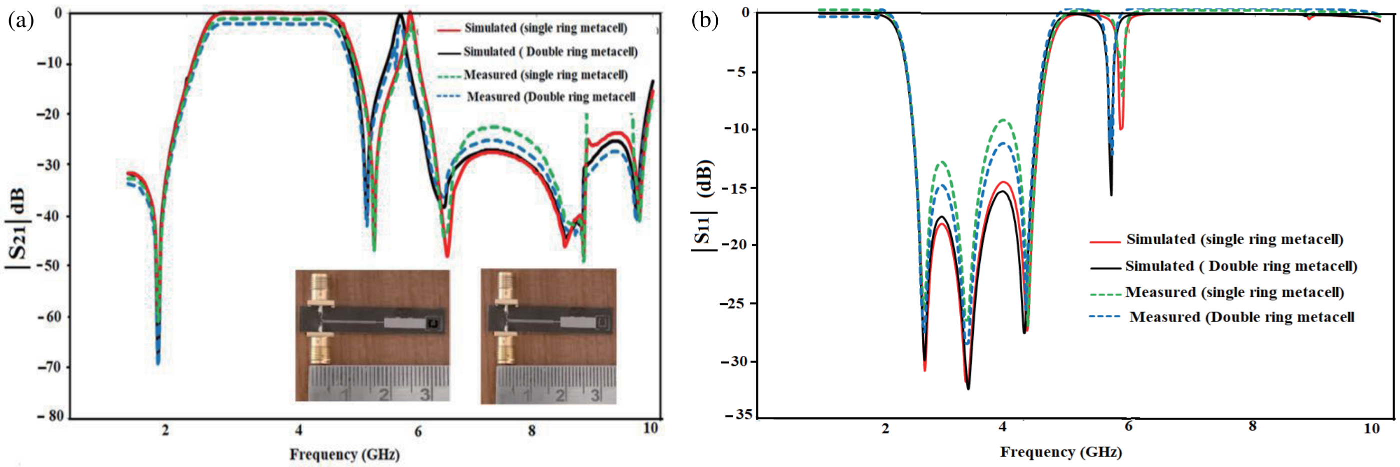


**FIGURE 5.** Experimental results (a) $S_{21}$ response. (b) $S_{11}$ response.

## 6. CONCLUSION

This article describes the successful design and implementation of a unique highly independent, controlled wide and narrow dual-band BPF. A multi-band response is obtained by using only two resonator structures. Moreover, our proposed filter has highly independent, controlled wide and narrow dual-band response. As the 5.7 GHz–5.8 GHz band is used as a common frequency band for point-to-multipoint spread spectrum communication system, high-speed wireless LAN, broadband wireless access system, Bluetooth technology equipment, and vehicle wireless automatic identification, our proposed filter is much suitable for these applications along with 5G communication.

## DECLARATION OF COMPETING INTEREST

The authors declare that they have no known competing financial interests or personal relationships that could have appeared to influence the work reported in this paper.


## ACKNOWLEDGEMENT

Authors would like to thank SAMEER — Center for Electromagnetics, Chennai, India for providing facility for testing and Measurement


## REFERENCES


[1] Xie, Y., F.-C. Chen, and Z. Li, "Design of dual-band bandpass filter with high isolation and wide stopband," *IEEE Access*, Vol. 5, 25 602–25 608, 2017.

[2] AbdulRehman, M. and S. Khalid, "Design of tri-band bandpass filter using symmetrical open stub loaded step impedance resonator," *Electronics Letters*, Vol. 54, No. 19, 1126–1127, Sep. 2018.

[3] Firmansyah, T., S. Praptodinoyo, R. Wiryadinata, S. Suhendar, S. Wardoyo, A. Alimuddin, C. Chairunissa, M. Alaydrus, and G. Wibisono, "Dual-wideband band pass filter using folded cross-stub stepped impedance resonator," *Microwave and Optical Technology Letters*, Vol. 59, No. 11, 2929–2934, Nov. 2017.

[4] Chu, Q.-X., F.-C. Chen, Z.-H. Tu, and H. Wang, "A novel crossed resonator and its applications to bandpass filters," *IEEE Transactions on Microwave Theory and Techniques*, Vol. 57, No. 7, 1753–1759, Jul. 2009.

[5] Killamsetty, V. K. and B. Mukherjee, "Miniaturised highly selective bandpass filter with very wide stopband using meander coupled lines," *Electronics Letters*, Vol. 53, No. 13, 889, Jun. 2017.

[6] Guo, X., L. Zhu, and W. Wu, "Design method for multiband filters with compact configuration in substrate integrated waveguide," *IEEE Transactions on Microwave Theory and Techniques*, Vol. 66, No. 6, 3011–3018, Jun. 2018.

[7] Zhou, K., C.-X. Zhou, H.-W. Xie, and W. Wu, "Synthesis design of SIW multiband bandpass filters based on dual-mode resonances and split-type dual- and triple-band responses," *IEEE Transactions on Microwave Theory and Techniques*, Vol. 67, No. 1, 151–161, Jan. 2019.

[8] Xu, J., W. Wu, and C. Miao, "Compact microstrip dual-/tri-/quad-band bandpass filter using open stubs loaded shorted stepped-impedance resonator," *IEEE Transactions on Microwave Theory and Techniques*, Vol. 61, No. 9, 3187–3199, Sep. 2013.

[9] Lee, C.-H., C.-I. G. Hsu, and H.-K. Jhuang, "Design of a new tri-band microstrip BPF using combined quarter-wavelength sirs," *IEEE Microwave and Wireless Components Letters*, Vol. 16, No. 11, 594–596, Nov. 2006.

[10] "A new tri-band bandpass filter for GSM WiMAX and ultrawideband responses by using asymmetric stepped impedance resonators," *Progress In Electromagnetics Research*, Vol. 124, 365–381, 2012.

[11] Mo, Y., K. Song, and Y. Fan, "Miniaturized triple-band bandpass filter using coupled lines and grounded stepped impedance resonators," *IEEE Microwave and Wireless Components Letters*, Vol. 24, No. 5, 333–335, May 2014.

[12] Chu, Q. and X. Lin, "Advanced triple-band bandpass filter using trisection SIR," *Electron. Lett.*, Vol. 44, No. 4, 4–5, 2008.

[13] Pelliccia, L., F. Cacciamani, and P. Farinelli, "High-Q tunable waveguide filters using IC RFMEMS switches," *IEEE Trans. Microw. Theory Tech.*, Vol. 63, No. 10, 3381–3390, 2015.

[14] Jiang, H., B. Lacroix, K. Choi, Y. Wang, A. T. Hunt, and J. Papapolymerou, "Ka- and U-band tunable bandpass filters using ferroelectric capacitors," *IEEE Transactions on Microwave Theory

*and Techniques*, Vol. 59, No. 12, 3068–3075, Dec. 2011.

[15] Zhao, G., B. You, X. Wen, and G. Luo, "A reconfigurable dual-band bandpass filter using memristive switches," *Journal of Electromagnetic Waves and Applications*, Vol. 36, No. 1, 115–130, Jan. 2022.

[16] Lu, D., N. S. Barker, and X. H. Tang, "Compact and independently-design tri-band bandpass filter with bandwidth and return loss control," *Electronics Letters*, Vol. 52, No. 24, 1992–1993, Nov. 2016.

[17] Chu, Q.-X., X.-H. Wu, and F.-C. Chen, "Novel compact tri-band bandpass filter with controllable bandwidths," *IEEE Microwave and Wireless Components Letters*, Vol. 21, No. 12, 655–657, Dec. 2011.

[18] Weng, M.-H., S.-W. Lan, S.-J. Chang, and R.-Y. Yang, "Design of dual-band bandpass filter with simultaneous narrow- and wide-bandwidth and a wide stopband," *IEEE Access*, Vol. 7, 147 694–147 703, 2019.

[19] Huang, C.-Y., M.-H. Weng, C.-Y. Hung, and S.-W. Lan, "Design of a dual-band bandpass filter for GSM and direct sequence ultra-wideband communication systems," *Journal of Electromagnetic Waves and Applications*, Vol. 25, No. 11-12, 1605–1615, 2011.

[20] Hugar, S., J. Baligar, V. Dakulagi, and P. Z. Alimovna, "Multiband bandpass filter with asymmetric dual-band response based on metacell," *Microwave and Optical Technology Letters*, Vol. 65, No. 12, 3126–3132, Dec. 2023.

[21] Bilotti, F., A. Toscano, and L. Vegni, "Design of spiral and multiple split-ring resonators for the realization of miniaturized metamaterial samples," *IEEE Transactions on Antennas and Propagation*, Vol. 55, No. 8, 2258–2267, Aug. 2007.

[22] Khani, S., S. M. H. Mousavi, M. Danaie, and P. Rezaei, "Tunable compact microstrip dual-band bandpass filter with tapered resonators," *Microwave and Optical Technology Letters*, Vol. 60, No. 5, 1256–1261, May 2018.

[23] Khani, S., M. Danaie, and P. Rezaei, "Miniaturized microstrip dual-band bandpass filter with wide upper stop-band bandwidth," *Analog Integrated Circuits and Signal Processing*, Vol. 98, No. 2, 367–376, Feb. 2019.

[24] Chen, J.-X., M.-Z. Du, Y.-L. Li, Y.-J. Yang, and J. Shi, "Independently tunable/controllable differential dual-band bandpass filters using element-loaded stepped-impedance resonators," *IEEE Transactions on Components Packaging and Manufacturing Technology*, Vol. 8, No. 1, 113–120, Jan. 2018.

[25] Gomez-Garcia, R., L. Yang, J.-M. Munoz-Ferreras, and D. Psychogiou, "Selectivity-enhancement technique for stepped-impedance-resonator dual-passband filters," *IEEE Microwave and Wireless Components Letters*, Vol. 29, No. 7, 453–455, Jul. 2019.

[26] Lalbakhsh, A., S. M. Alizadeh, A. Ghaderi, A. Golestanifar, B. Mohamadzade, M. B. Jamshidi, K. Mandal, and W. Mohyuddin, "A design of a dual-band bandpass filter based on modal analysis for modern communication systems," *Electronics*, Vol. 9, No. 11, 1770–1779, Nov. 2020.

[27] Weng, M.-H., S.-W. Lan, S.-J. Chang, and R.-Y. Yang, "Design of dual-band bandpass filter with simultaneous narrow- and wide-bandwidth and a wide stopband," *IEEE Access*, Vol. 7, 147 694–147 703, 2019.

[28] Chen, C.-F., G.-Y. Wang, and J.-J. Li, "Compact microstrip dual-band bandpass filter and quad-channel diplexer based on quint-mode stub-loaded resonators," *IET Microwaves Antennas & Propagation*, Vol. 12, No. 12, 1913–1919, Oct. 2018.